Available online at www.sciencedirect.com
SCIENCE DIRECT®
Bioorganic & Medicinal Chemistry 13 (2005) 1913–1922
Bioorganic & Medicinal Chemistry

Cooperative lectin recognition of periodical glycoclusters along DNA duplexes: alternate hybridization and full hybridization

Yoshinao Yamada,[a] Kazunori Matsuura[b] and Kazukiyo Kobayashi[a,*]

[a]*Department of Molecular Design and Engineering, Graduate School of Engineering, Nagoya University, Nagoya 464-8603, Japan*
[b]*Department of Chemistry and Biochemistry, Graduate School of Engineering, Kyushu University, Hakozaki, Fukuoka 812-8581, Japan*

Received 28 October 2004; revised 14 January 2005; accepted 14 January 2005

Abstract—We describe herein the construction of periodically, spatially controlled glycoclusters along DNA duplexes and their cooperative lectin recognition. Site-specifically α-mannosylated oligodeoxynucleotide 20-mer (Man-ODN20) was synthesized via the phosphoramidite solid-phase synthesis. Alternate hybridization of the Man-ODN20 with the half-sliding complementary ODN 20-mer (hscODN20) gave an alternately prolonged Man-cluster Man-ODN20/hscODN20. The binding of the Man-cluster to FITC-labeled ConA lectin showed sigmoidal fluorescence dependency on the concentration of Man-ODN, indicating that some mannose residues along the repeating DNA duplex were cooperatively bound to ConA (apparent affinity constant: $K_{af} = 2.4 \times 10^4$ M^{-1} and Hill coefficient: $n = 3.5$). The duplex of Man-ODN20 with full complementary ODN 20-mer (fcODN20) was little bound to ConA. The binding behavior of Man-ODN20/hscODN20 is compared with that of the alternately prolonged Gal-cluster Gal-ODN20/hscODN20 previously reported. Duplexes 20-mer, 40-mer, and 60-mer presenting one, two, and three periodic galactoses were also prepared by full hybridization of 20-mer β-galactosylated oligodeoxynucleotide (Gal-ODN20) with the periodically repeating full complementary 20-mer, 40-mer, and 60-mer ODNs. RCA_{120} lectin was found to little bind the 20-mer and 40-mer duplexes and to bind weakly and non-cooperatively the 60-mer duplex ($K_{af} = 1.1 \times 10^4$ M^{-1}). The cooperative lectin recognition of these glycoclusters in relation with the degree of association (DA) of ODN and the numbers of glycosides along the DNA duplex is discussed.

1. Introduction

Cell surface glycoconjugates are essential in mediating and modulating cell adhesion and cellular signaling.[1,2] It is well known that these biological functions usually result from carbohydrate–lectin interactions and that the interactions are greatly enhanced by the multivalency or glycocluster effect of the glycoconjugates.[3] How to express effectively the glycocluster effect is the most basic guideline for molecular design of specialty glycoconjugate substances and materials. There have been reported various types of glycoconjugate polymers,[4,5] dendrimers,[6] calixarenes,[7] cyclodextrins,[8] transition metal complexes,[9] liposomes,[10] and monolayers at air–water interface.[11] However, there has been little success in control of the intervals and directions of the carbohydrates along the scaffolds.[12]

As illustrated in Figure 1A, we have proposed a novel concept, 'half-sliding' complementary oligodeoxynucleotide (hscODN), to give spatially, periodically controlled glycoclusters along a DNA duplex.[13] The glycosylated ODN 20-mer and the hscODN 20-mer were synthesized in an automated synthesizer. The left 10-mer half-sequence of the hscODN (blue) is designed to be complementary to the right 10-mer half-sequence of the glycosylated ODN (blue). Also, the right 10-mer half-sequence of the hscODN (red) is designed to be complementary to the left 10-mer half-sequence (red) of the glycosylated ODN. When the glycosylated ODN and the hscODN are mixed, the respective complementary sequences are subjected to alternate hybridization to extend the self-organization along the DNA duplex. As the result, the carbohydrate signals are arranged at regular intervals and in the same direction to yield the periodic and directional glycocluster.

Keywords: Glycoclusters; Recognition; Oligonucleotides; Self-organization.
* Corresponding author. Tel.: +81 52 789 2488; fax: +81 52 789 2528; e-mail: kobayash@mol.nagoya-u.ac.jp

0968-0896/$ - see front matter © 2005 Elsevier Ltd. All rights reserved.
doi:10.1016/j.bmc.2005.01.021

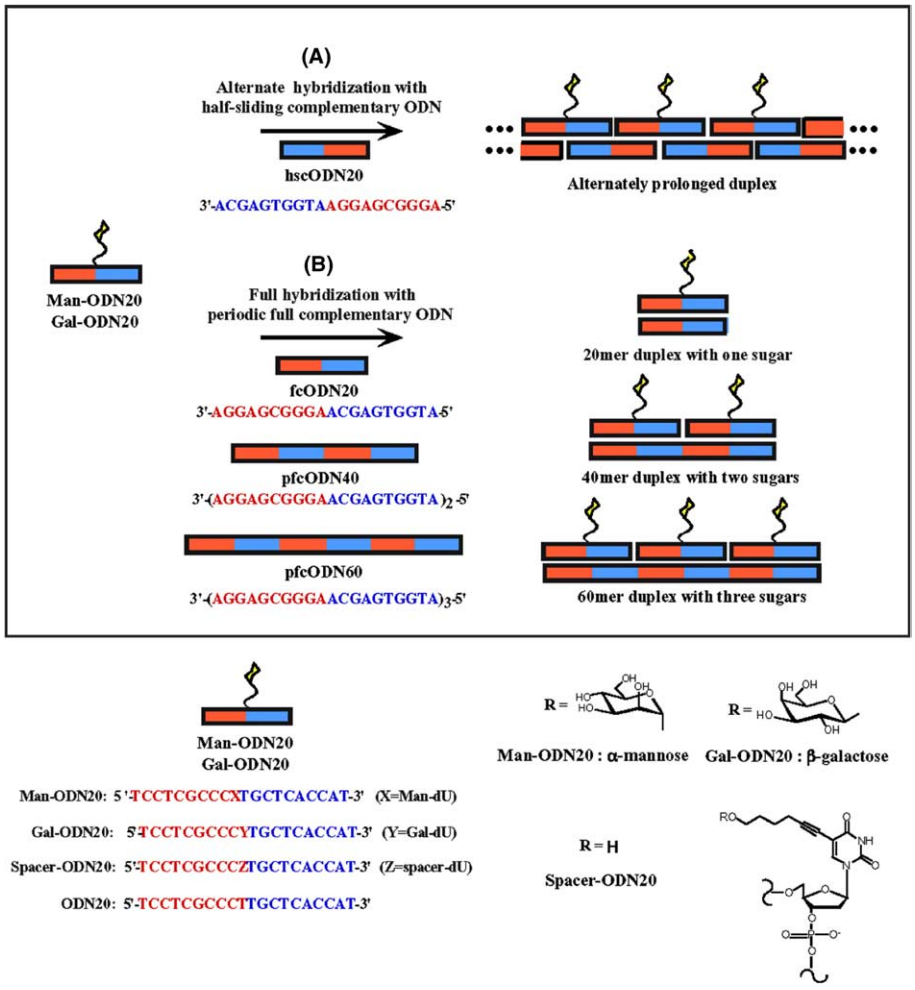

Figure 1. Construction of the two distinct types of periodic glycoclusters. (A): Alternate hybridization between glyco-ODN (20-mer) and half sliding complementary ODN (hsc-ODN) (20-mer) gave a periodically prolonged glycocluster along DNA duplex. (B): Full hybridization between glyco-ODN (20-mer) and periodically repeating full complementary ODNs (1×20-mer, 2×20-mer, and 3×20-mer) gave periodical glycoclusters along DNA duplexes with constant lengths. The red and blue sequences of the target sugar-ODNs are complementary, respectively, to the red and blue sequences of the corresponding template ODNs.

The present study has attempted to develop the 'half-sliding' or 'alternate hybridization' concept extensively and to gain deep understanding of the cooperative lectin recognition.[14] Figure 1 lists the oligodeoxynucleotides used in this paper. First, the target of hsc-ODN 20-mer (hscODN20) was extended to α-D-mannosylated ODN (Man-ODN20: the center of 20-mer ODN was modified) to compare with the previously reported β-D-galactosylated ODN (Gal-ODN20: the center of 20-mer ODN was modified). Comparison is also made with non-glycosylated natural ODN (ODN20), and hydroxy-alkyne-modified ODN with the spacer but without a glycoside residue (Spacer-ODN20). The second category (Fig. 1B) includes full complementary 20-mer (fcODN20) to the glycosylated 20-mer ODN and its periodically repeating full complementary 40-mer (pfcODN40) and 60-mer (pfcODN60). Full hybridization of Gal-ODN20 with these 20-mer, 40-mer, and 60-mer ODNs yielded periodic glycoclusters along DNA duplexes carrying one, two, and three galactose residues. In this paper, we use different representations for these two types of duplexes: the duplex Man-ODN20/hscODN20 underlined for the alternate hybridization and the duplex {Man-ODN20/fcODN20} in braces for the full hybridization. Recognition of these glycoclusters to α-Man-specific concanavalin A (ConA) and β-Gal-specific RCA_{120} is estimated quantitatively by fluorometry. The relationship between these glycoclusters and lectin recognition is discussed.

2. Results

2.1. Synthesis of α-mannosylated ODN (Man-ODN20)

Scheme 1 shows the synthesis of α-mannose-modified deoxyuridine phosphoramidite derivative **7**. The yield of product **4** (78%) in the Heck reaction was higher than that of the corresponding galactose derivative (58%).[15] Solid-phase synthesis of Man-ODN20 was performed on an automated system from the 3′ to 5′ end by using benzimidazolium triflate[16] as an activator in 1 μmol scale. The ODNs were deprotected and then purified by HPLC with >99% purity. The HPLC retention time

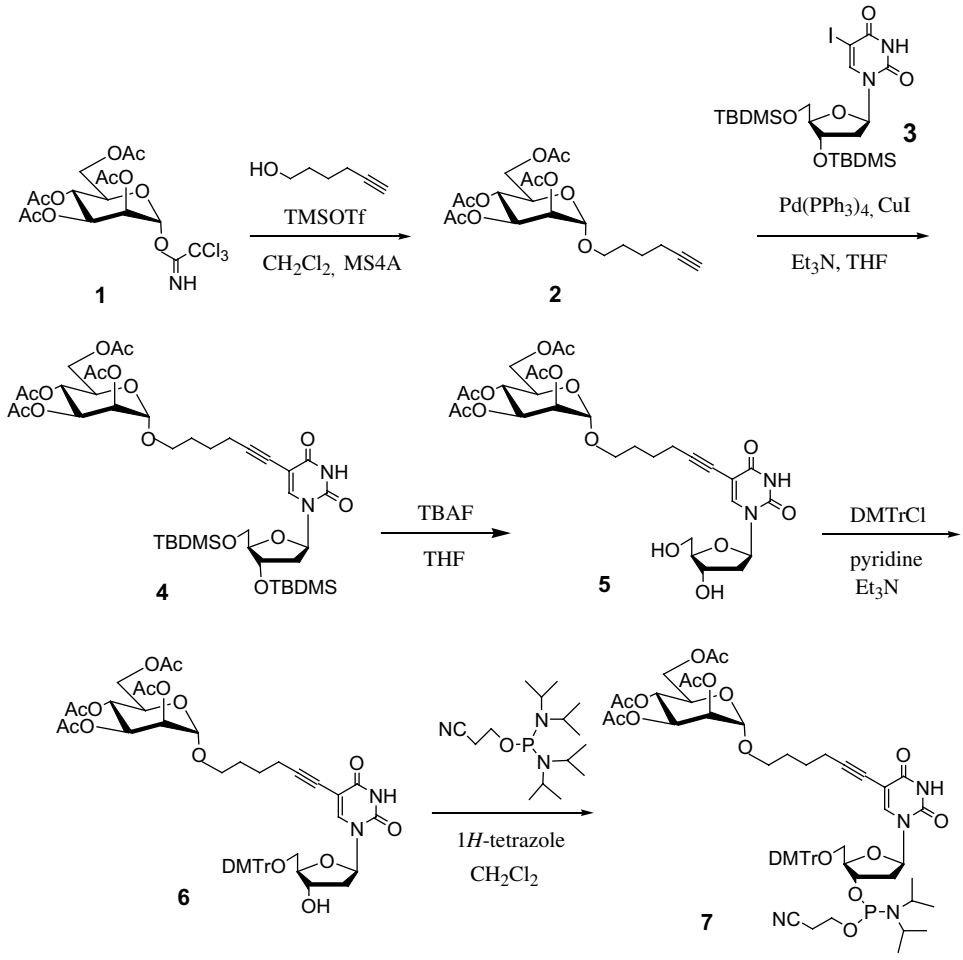

Scheme 1. Synthesis of α-mannose-modified deoxyuridine derivatives.

of Man-ODN20 was the same as that of Gal-ODN20, which was confirmed by MALDI-TOF MS. Man-ODN20 was obtained with about 40% total coupling efficiency as judged by HPLC.

The total coupling efficiency of Man-ODN20 was lower than that of the corresponding Gal-ODN20 (70–80%). Phosphoramidite addition was monitored by the orange color of the trityl cation released at the detritylation step. It was observed that the phosphoramidite addition was depressed at the step immediately after the Man-modified unit. The main byproduct was the 10-mer ODN with a terminal mannosylated residue (50–60%). It is possible that the α-Man-modified deoxyuridine derivative, compared with the β-Gal-modified one, may take a disadvantageous steric arrangement towards the addition of the subsequent phosphoramidite.

2.2. CD and melting behaviors

Figure 2 illustrates the representative CD spectra of various types of duplexes constructed via alternate hybridization and full hybridization. These CD spectra are similar to the typical B-type conformation, suggesting that these glycoclusters composed of both alternately and fully hybridized duplexes take the B-type conformation.

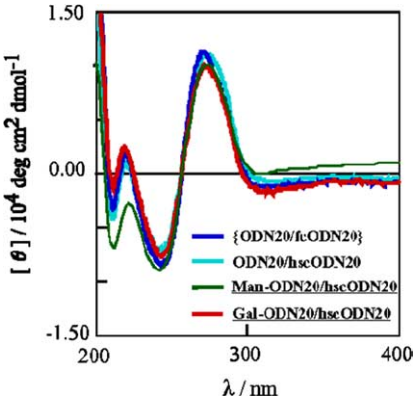

Figure 2. CD spectra of the duplexes of Man-ODN20 and Gal-ODN20 with hscODN20 at [ODN] = 1.13 μM in PBS (pH 7.4) at 25 °C.

The melting temperatures (T_m) of the duplexes were estimated from the hyperchromicity curves at [ODN] = 1.13 μM in PBS (pH 7.4). The T_m data of the 20-mer duplexes constructed via full hybridization are as follows: {Man-ODN20/fcODN20} (69 °C) ≅ {Spacer-ODN20/fcODN20} (69 °C) > {ODN20/fcODN20} (68 °C) > {Gal-ODN20/fcODN20} (65 °C). The T_m of {Man-ODN20/fcODN20} duplex and {Spacer-ODN20/

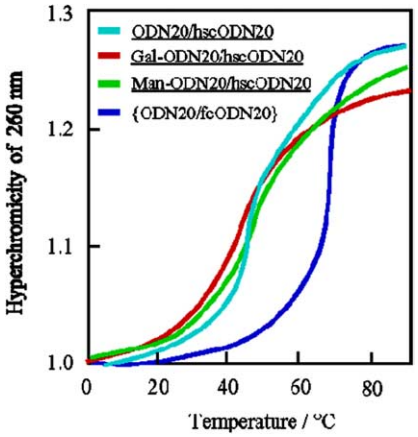

Figure 3. Melting behaviors of the duplexes of Man-ODN20 and Gal-ODN20 with hscODN20 at [ODN] = 1.13 μM in PBS (pH 7.4).

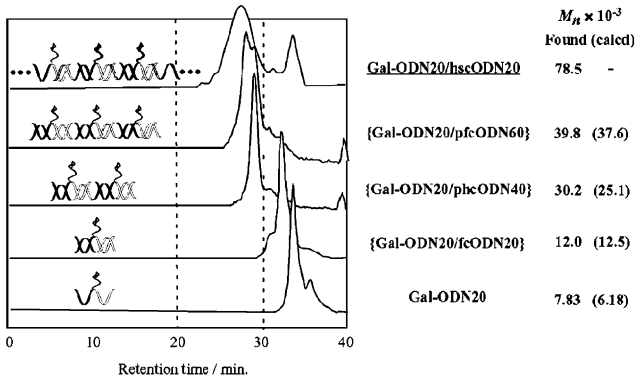

Figure 4. Size-exclusion chromatography of Gal-cluster duplexes. Shodex OH Pak SB-804 HQ to SB-803 HQ column, eluent: PBS buffer (pH 7.4) at 25 °C, flow rate: 0.5 mL/min, standard: pullulan.

fcODN20} duplex were a little higher than that of {ODN20/fcODN20} duplex. As reported previously,[15] the alkyne was conjugated with the pyrimidine ring to enhance the stacking of the base and to result in the stabilization of the duplex.[17] It is noted that the T_m of {Gal-ODN20/fcODN20} duplex was lower by 3 °C than that of {ODN20/fcODN20} duplex. The Gal derivative slightly destabilized the duplex but the Man derivative little affected the stability of the duplex.

The melting behaviors of the alternately prolonged duplexes are compared in Figure 3. The T_ms of Man-ODN20/hscODN20 (45 °C), Gal-ODN20/hscODN20 (45 °C), and ODN20/hscODN20 (46 °C) were similar, but about 20 °C lower than that of full complementary duplex {ODN20/fcODN20} (68 °C). It is known that the stacking of nucleic acid base pairs is distorted at the chain end of a DNA duplex. Hence, it is reasonable that the distortion of stacking was increased in the alternately prolonged duplexes to result in lowering the stability and melting temperature. Nevertheless, the alternate hybridization keeps the duplex structure near the room temperature, which is important in investigating the lectin recognition of these alternately prolonged duplexes at 25 °C.

2.3. Estimation of molecular size by SEC

Figure 4 compares the size-exclusion chromatography (SEC) of the glycoclusters along DNA duplexes constructed via alternate hybridization and full hybridization. We employed Gal-ODN20 in this experiment: Gal-ODN20 and hscODN20 for alternate hybridization and Gal-ODN20 and periodic full complementary ODNs (pfcODN60, pfcODN40, and fcODN20) for full hybridization. The apparent molecular size and its distribution estimated with pullulan standards are listed as M_n and M_w/M_n, respectively. The apparent molecular sizes were increased as follows. The single strand 20-mer ODN (Gal-ODN20) (M_n = 7830, M_w/M_n = 1.04) < the full complementary 20-mer duplex {Gal-ODN20/fcODN20} (M_n = 12,000, M_w/M_n = 1.05) < the periodic full complementary 40-mer duplex {Gal-ODN20/pfcODN40} (M_n = 30,100, M_w/M_n = 1.02) < the periodic full complementary 60-mer duplex {Gal-ODN20/pfcODN60} (M_n = 39,800, M_w/M_n = 1.06) < the alternately prolonged duplex Gal-ODN20/hscODN20 (M_n = 78,500, M_w/M_n = 1.89). The values of the full complementary 20-mer, 40-mer, and 60-mer duplexes are close to the corresponding calculated molecular weights.

The average degree of association (DA) of the alternately prolonged duplex was estimated to be about 12.6. This suggests that about 6.3 galactosides were assembled on the alternately prolonged duplex. As will be described in the Discussion section, the thermodynamic treatment (Fig. 8b) gave the average DA of the alternately prolonged duplex to be about 13.9 at the same ODN concentration ([ODN] = 85 μM). It is possible that the slightly smaller DA value from SEC is caused by the partial dissociation of the duplex diluted during the SEC elution, as suggested by the SEC diagram in which some dissociated product was eluted at the longer retention time. It is also noted that the alternately prolonged duplexes Gal-ODN20/hscODN20 and Man-ODN20/hscODN20 are considered to form similar size glycoclusters.

2.4. Binding of glycoclusters with lectins

Binding affinity was estimated quantitatively by fluorometry with FITC-labeled α-Man-specific FITC-ConA (Fig. 5) and β-Gal-specific FITC-RCA_{120} (Fig. 6). The fluorescence intensity change ($\Delta F/F_0$) of the FITC-labeled lectin was recorded at 518 nm (excitation wavelength: 490 nm) with an increasing amount of ODN. As shown in Figure 5, the alternately prolonged duplex of Man-ODN with half-sliding complementary ODN Man-ODN20/hscODN20 increased significantly the fluorescence spectral change to give a steep sigmoidal curve. In contrast, the fluorescence intensity of the duplex of Man-ODN with full complementary ODN {Man-ODN20/fcODN20} as well as the duplex of unmodified ODN with half-sliding complementary ODN ODN20/hscODN20 little increased in the present concentration range.

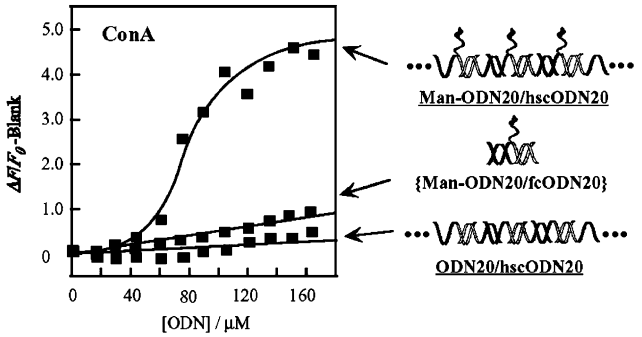

Figure 5. Interaction between Man-ODN20 and ConA. Dependency of fluorescence intensity of FITC-ConA at 518 nm (excitation wavelength: 490 nm) on the concentration of ODNs in PBS (pH 7.4) at 25 °C. [ConA] = 14.6 nM, [Man] = 0–82.5 μM.

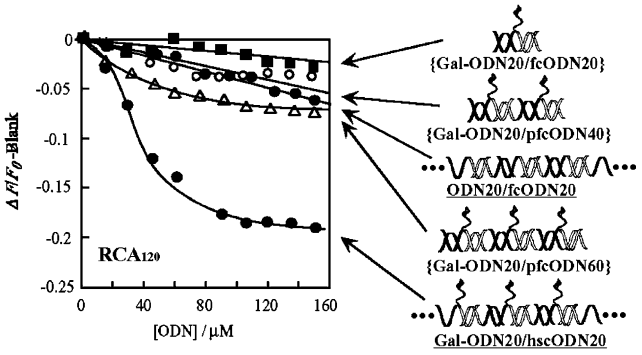

Figure 6. Interaction between Gal-ODN20 and RCA_{120}. Dependency of fluorescence intensity of FITC-RCA_{120} at 518 nm (excitation wavelength: 490 nm) on the concentration of ODNs in PBS (pH 7.4) at 25 °C, [RCA_{120}] = 14.6nM, [Gal] = 0–75 μM.

As reported previously,[13,14] the alternately prolonged duplex Gal-ODN20/hscODN20 also increased significantly the fluorescence spectral change with a steep sigmoidal curve (Fig. 6). In contrast, the double strand 60-mer {Gal-ODN20/pfcODN60} with three galactoses gave a saturated binding curve, while the double strand 40-mer {Gal-ODN20/pfcODN40} with two galactoses as well as the 20-mer {Gal-ODN20/fcODN20} with one galactose were found to change little the fluorescence.

It may be noted that FITC-ConA yielded the positive $\Delta F/F_0$ curve and FITC-RCA_{120} yielded the negative $\Delta F/F_0$ curve. We often encountered negative $\Delta F/F_0$ curves of FITC-lectins bound to glycoconjugate polymers.[18] The fluorescence change depends on many factors including molecular motion and hydration in the environment of the lectins, which complicates elucidation of the fluorescence change.

These fluorescence changes were treated with the Hill equation (Eq. 1) to obtain the apparent affinity constant (K_{af}) and the Hill coefficient (n).

$$\log(Y/(1-Y)) = n\log[\text{Sugar}] + n\log K_{af} \times (Y = \Delta F/\Delta F_{max}) \quad (1)$$

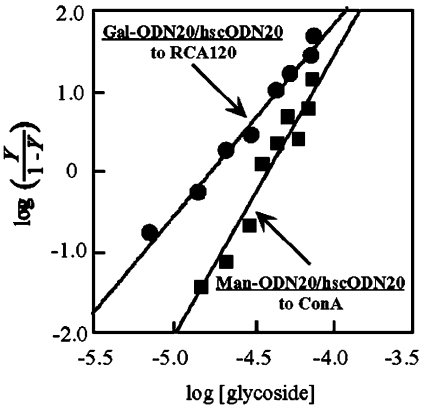

Figure 7. Hill plots of the fluorescence intensity change of FITC-ConA with Man-cluster and FITC-RCA_{120} with Gal-cluster.

As plotted in Figure 7, the alternately prolonged duplexes of the mannose cluster Man-ODN20/hscODN20 and the galactose cluster Gal-ODN20/hscODN20 gave the linear relationship on the Hill equation. Man-ODN20/hscODN20 for ConA: $K_{af} = 2.4 \times 10^4\ M^{-1}$ and $n = 3.5$. Gal-ODN20/hscODN20 for RCA_{120}: $K_{af} = 5.5 \times 10^4\ M^{-1}$ and $n = 2.4$.[13] Although the binding of the 60-mer double strand {Gal-ODN20/pfcODN60} (with three galactoses) was not sigmoidal and hence not cooperative, an estimation based on the Hill equation with $n = 1$ gave $K_{af} = 1.1 \times 10^4\ M^{-1}$.

3. Discussion

We discuss here the cooperative lectin recognition of these glycoclusters in relation with the degree of association or hybridization (DA) of ODN and the numbers of glycosides along the DNA duplex. Hybridization is a thermodynamic equilibrium process depending on the concentration of the ODN. Previously, we estimated the degree of association (DA) of alternate hybridization on the basis of the thermodynamic treatment of T_ms as follows. The T_ms of the alternate hybridization Gal-ODN20/hscODN20 were determined at several concentrations. From the linear relationship of the $1/T_m$ against the logarithm of the concentrations, we obtained the apparent association or hybridization constant $K_{as} = 4.2 \times 10^6\ M^{-1}$ at 25 °C and the thermodynamic parameters ($\Delta G^o = -9.0 \times 10^4$ kcal mol^{-1}; $\Delta H^o = -44$ kcal mol^{-1}; $\Delta S^o = -120$ cal mol^{-1} K^{-1}). It should be pointed out that K_{as} for hybridization is much larger (>10^2) than K_{af} for lectin affinity. The degree of association (DA) of the alternate hybridization Gal-ODN20/hscODN20 is given by Eq. 2,[19,20] where DA depends on the K_{as} and the total ODN concentration C/M.[21]

$$DA = \frac{K_{as}C}{\sqrt{2K_{as}C+1}-1} \quad (2)$$

Figure 8B illustrates the dependency of the DA on the total ODN concentration. The dependency is applicable to both Gal-ODN20/hscODN20 and Man-ODN20/hscODN20 since both had the same T_m (45 °C at [ODN] = 1.13 μM). The fluorescence change of the

bound Con A (Fig. 8A) and RCA_{120} (Fig. 8C) against the total ODN concentrations can be discussed on the basis of DA. The binding ability of the mannose cluster to ConA is enhanced significantly at about 80 μM ODN, which corresponds to DA = about 13.5 as the dotted line shows. This suggests that about seven mannosides on the alternately prolonged duplex lead to the cooperative binding to ConA. On the other hand, the binding ability of the galactose cluster to RCA_{120} is enhanced significantly at about 40 μM ODN, which corresponds to DA = about 9.7, suggesting that about five galactosides lead to the cooperative binding to RCA_{120}. Compared with RCA_{120}, ConA requires a larger number of carbohydrates along the DNA duplex for the cooperative binding. Furthermore, the fluorescence intensity changes ($\Delta F/F_0$) of FITC-ConA and FITC-RCA_{120} were saturated, respectively, at about 150 μM ODN and at about 100 μM ODN, which correspond to about nine mannosides and to about 7–8 galactosides on the respective alternately prolonged duplexes.

α-Mannose specific lectin (ConA) strongly recognized the periodical mannose cluster Man-ODN20/hscODN20 constructed via alternate hybridization. The Hill coefficient ($n = 3.5$) suggests that 3.5 mannose residues on the average were cooperatively bound to the four binding sites on the tetrameric ConA lectin. The distance between the binding sites of ConA (about 65 Å)[22] is close to the interval (68 Å) of the mannose residue located at every 20 bases along the DNA duplex, so we assume that the mannose residues were able to be bound to 3–4 binding sites of ConA. RCA_{120} also strongly recognized the periodical galactose cluster Gal-ODN20/hscODN20. The Hill coefficient ($n = 2.4$) suggests that 2.4 galactose residues on the average were cooperatively bound to the three binding sites on the tetrameric RCA_{120} lectin.

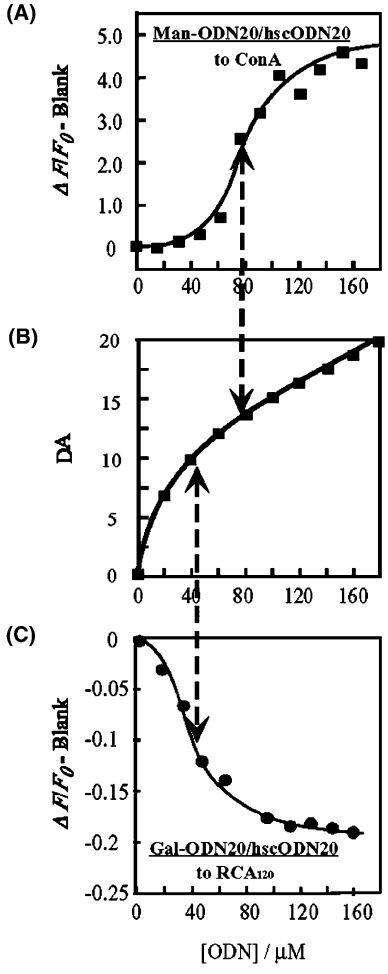

Figure 8. Dependency of the lectin binding (A: Con A and C: RCA_{120}) and the DA (B) of the alternately hybridized periodical glycoclusters on the total ODN concentration. The dotted line indicates the DA of ODN, which corresponds to the inflection point of the sigmoidal curve.

The periodic 60-mer full complementary duplex {Gal-ODN20/pfcODN60} was bound to RCA_{120} lectin weakly and non-cooperatively. On the other hand, the alternately prolonged duplex Gal-ODN20/hscODN20 required about five galactosides to induce its cooperative binding to RCA_{120}. The length of periodic full complementary duplexes is fixed, but the length of alternately prolonged duplexes depends on the concentration of the ODN. We assume that alternately prolonged duplexes are rather flexible to be bound to the corresponding lectins cooperatively, but this assumption remains to be verified. These characteristics must be compared between alternately prolonged duplexes and periodic full complementary duplexes carrying constant numbers of carbohydrates in precise distance. It is also of interest to prepare periodic duplexes via ligation of both alternately prolonged duplexes and periodic full complementary duplexes.

4. Conclusion

We have prepared spatially, periodically controlled Man-clusters along DNA duplexes via alternate hybridization and evaluated their lectin recognition in comparison with those of Gal-clusters prepared via alternate hybridization and full hybridization. Whereas the periodic 40-mer Gal-cluster {Gal-ODN20/pfcODN40} with two galactosides was minimally recognized by RCA_{120}, the periodic 60-mer Gal-cluster {Gal-ODN20/pfcODN60} with three galactosides was recognized weakly and non-cooperatively by RCA_{120} ($K_{af} = 1.1 \times 10^4\ M^{-1}$). On the other hand, alternate hybridization of Man-ODN and Gal-ODN with the half-sliding complementary ODN (hsc-ODN) gave the sigmoidal fluorescence dependency on the total ODN concentration. The analysis for the cooperative recognition using the Hill equation yielded the following affinity constants. $K_{af} = 2.4 \times 10^4\ M^{-1}$ and $n = 3.5$ for Man-ODN20/hscODN20 and ConA. $K_{af} = 5.5 \times 10^4\ M^{-1}$ and $n = 2.4$ for Gal-ODN20/hscODN20 and RCA_{120}.

The cooperative lectin recognition of these glycoclusters in relation with the degree of association (DA) of ODN and the numbers of glycosides along the DNA duplexes was discussed. According to our estimation, about seven mannose residues and about five galactose residues on the alternately prolonged duplexes led to the cooperative

binding, respectively, to ConA and to RCA_{120}. Compared with RCA_{120}, ConA required a larger number of carbohydrates along the DNA duplex for the cooperative binding.

Alternate hybridization using a half-sliding complementary ODN has enabled us to control the intervals and directions of the carbohydrates along the scaffolds. We expect that this strategy of 'assembly-amplified cooperative molecular recognition' will contribute to the development of both DNA nanotechnology and glyco-nanotechnology using periodical glycoclusters along DNA duplexes.

5. Experimental

5.1. General methods

^{1}H NMR spectra were recorded on a Varian INOVA-500 (500 MHz) at ambient temperature using tetramethylsilane and residual non-deuterated solvents as internal references. Absorption spectra were taken on a JASCO V-530 spectrophotometer equipped with a thermal controller. CD spectra were taken in a 10 mm quartz cell with a JASCO J-720 L spectrophotometer. Fluorescence spectra were recorded on a JASCO FP-777 spectrophotometer equipped with a thermal controller. Solid-phase syntheses of ODNs were conducted on an Expedite Nucleic Acid Synthesis System. Size-exclusion chromatography (SEC) was recorded with a JASCO Gulliver system equipped with SB-804HQ to SB-803HQ columns and a RI detector (RI-930) using 0.1 M phosphate buffer (pH 7.0) as eluent and pullulan as standards at 25 °C. Reversed phase high-performance liquid chromatography (HPLC) was recorded with a Shiseido Capcell Pak C18 UG120 column (4.5 × 150 mm) and a JASCO Gulliver UV/VIS detector (UV-975) at 25 °C. Merck precoated TLC plates (silica gel 60-F254, layer thickness 0.25 mm) were used for thin layer chromatography (TLC). The products were purified by preparative column chromatography on silica gel (Merck Art. No7734, 70–230 mesh).

5.2. Materials

Reactions sensitive to moisture and air were performed under nitrogen or argon atmosphere using anhydrous solvents and reagents. The following five types of ODNs were purchased from Rikaken Co., Ltd (Nagoya): unmodified 20-mer (ODN20: 5′-TCC TCG CCC TTG CTC ACC AT-3′), full complement 20-mer (fcODN 20: 5′-ATG GTG AGC AAG GGC GAG GA-3′), half-sliding cDNA 20-mer (hscODN20: 5′-AGG GCG AGG AAT GGT GAG CA-3′), periodic full cDNA 40-mer (pfcODN40: 5′-(ATG GTG AGC AAG GGC GAG GA)$_2$-3′), periodic full cDNA 60-mer (pfcODN60: 5′-(ATG GTG AGC AAG GGC GAG GA)$_3$-3′). Fluorescein isothiocyanate (FITC) labeled *Ricinus communis* agglutinin (FITC-RCA_{120}) and concanavalin A (FITC-ConA, from *Canavalia ensiformis*) were purchased from Sigma Co., Ltd. All other chemicals for the synthesis were purchased from Sigma Co., Ltd, Aldrich Chemical Company, Inc., and Tokyo Chemical Industry Co., Ltd.

5.3. (5-Hexyn-1-yl) 2,3,4,6-tetra-*O*-acetyl-α-D-mannopyranoside (2)

5-Hexyn-1-ol (170 mL, 1.5 mmol) was added to a solution of 2,3,4,6-tetra-*O*-acetyl-D-mannosyl trichloroacetimidate **1** (0.5 g, 1.0 mmol) and MS4A in 10 mL of CH_2Cl_2. The mixture was stirred under nitrogen at room temperature for 2 h. TMSOTf (58 mL, 0.3 mmol) was added at −40 °C. The resulting mixture was stirred at 0 °C for 30 min and at room temperature for 12 h. After removal of the molecular sieves by filtration, the filtrate was extracted with chloroform (×3) and the organic layer was washed with satd $NaHCO_3$ aq (×2) and water (×2). After drying over anhydrous $MgSO_4$, chloroform was evaporated to provide a thick oil. Purification by silica gel column chromatography eluting with toluene/AcOEt (5:1) provided pure **2** as a light yellow oil. Yield 0.23 g, 54.2%; ^{1}H NMR (500 MHz, $CDCl_3$): δ 5.35 (1H, d, J=3.5 Hz, 4-H), 5.31 (1H, dd, J = 3.5 Hz, 10.0, 2-H), 5.25 (1H, d, J = 10.5 Hz, 3-H), 4.81 (1H, d, 1-H), 4.33–4.10 (2H, m, 6-H), 3.73–3.70 (1H, m, C1–OC*H*H), 3.99–3.97 (1H, m, 5-H), 3.48–3.52 (1H, m, C1–OCH*H*), 2.23–2.26 (2H, m, CH_2−C≡CH), 2.16, 2.11, 2.05, 2.00 (12H, 4s, $OCOCH_3$), 1.97 (1H, t, C≡CH), 1.77–1.75 (2H, m, CH_2–CH_2–CH_2–C≡CH) and 1.63–1.58 ppm (2H, m, CH_2–CH_2–CH_2–C≡CH).

5.4. 5-Iodo-2′-deoxyuridine 3′,5′-di-*tert*-butyldimethylsilyl ether (3)

A solution of *tert*-butyldimethylsilyl chloride (3.2 g, 21.2 mmol) in 7 mL of dry DMF was added to a solution of anhydrous imidazole (2.4 g, 35.0 mmol) in 7 mL of dry DMF in an ice-water bath. After stirring for 10 min, D-5-iodo-2′-deoxyuridine (2.5 g, 7.1 mmol) in 6 mL of dry DMF was added to the solution under nitrogen at 0 °C. The mixture was stirred at room temperature for 3 h, and then the reaction mixture was quenched by addition of water. The residue was extracted with diethyl ether (×3) and the organic layer was washed with brine (×3) and water (×3). After drying over anhydrous $MgSO_4$, ether was evaporated to provide a thick oily substance. Purification by silica gel column chromatography eluting with hexane/AcOEt (4:1) provided pure **3** as a colorless foam. Yield 4.1 g, 99.8%; ^{1}H NMR (500 MHz, $CDCl_3$): δ 8.35 (1H, br, NH), 8.12 (1H, s, 6-H), 6.3 (1H, dd, J = 9.0, 6.0 Hz, 1-H), 4.43–4.41 (1H, m, 3′-H), 4.02–4.00 (1H, m, 4′-H), 3.92 (1H, dd, J = 12.0, 3.0 Hz, 5′-H), 3.78 (1H, dd, J = 12.0, 3.0 Hz, 5″-H), 2.40–2.28 (1H, m, 2′-*H*H), 2.08–1.96 (1H, m, 2′-H*H*), 0.97 (9H, s), 0.92 (9H, s), 0.18 (3H, s), 0.17 (3H, s), 0.11 (3H, s), and 0.10 ppm (3H, s).

5.5. 5-((2,3,4,6-Tetra-*O*-acetyl-α-D-mannopyranosyloxy)-hexyn-1-yl)-2′-deoxyuridine 3′,5′-di-tert-butyldimethylsilyl ether (4)

To a solution of **3** (64 mg, 0.11 mmol) and MS4A in 1.5 mL of dry THF were added $Pd(PPh_3)_4$ (12.7 mg,

0.011 mmol), CuI (4.2 mg, 0.022 mmol), Et_3N (30.5 mL, 0.22 mmol), and **2** (140 mg, 0.33 mmol) in 1.5 mL of dry THF under nitrogen. The mixture was stirred at room temperature for 26 h. After removal of the molecular sieves by filtration, the filtrate was extracted with AcOEt and washed with satd $NaHCO_3$ aq (×2) and water (×2). After drying over anhydrous $MgSO_4$, AcOEt was evaporated to provide a thick oil. Purification by silica gel column chromatography eluting with hexane/AcOEt (5:3 to 1:1) to provide pure **4** as a light yellow oil. Yield 75.9 mg, 78.2%; ^{1}H NMR (500 MHz, $CDCl_3$): δ 7.89 (1H, s, 6-H), 6.26 (1H, t, 1′-H), 5.30–5.20 (3H, m, J = 3.0 Hz, 4″-H, 2″-H, 3″-H), 4.78 (1H, d, J = 1.5 Hz, 1″-H), 4.40–4.38 (1H, m, 3′-H), 4.25–4.08 (2H, m, 6″-HH), 3.95–3.94 (2H, m, 4′, 5′-H), 3.87 (1H, d, J = 2.0 Hz, 5″-H), 3.75 (2H, m, 5′-H, C1–O–CHH), 3.46 (1H, m, C1–O–CH*H*), 2.40–2.26 (4H, m, 2′-HH, CH_2–CH_2–C*H*$_2$–C≡C), 2.14, 2.07, 2.00, 1.96 (12H, 4s, $OCOCH_3$), 1.72–1.73 (2H, m, C*H*$_2$–CH_2–CH_2–C≡C), 1.64–1.63 (2H, m, CH_2–C*H*$_2$–CH_2–C≡C), 0.81 (s, 9H), 0.88–0.86 (s, 9H), 0.05–0.07 (s, 6H), and 0.10 ppm (s, 6H).

5.6. 5-((2,3,4,6-Tetra-*O*-acetyl-α-D-mannopyranosiloxy)-hexyn-1-yl)-2′-deoxyuridine (5)

A solution (1.0 M) of tetrabutylammonium fluoride (1.09 mL, 1.09 mmol) in dry THF was added to a solution of **4** (320 mg, 0.36 mmol) in 10 mL of dry THF under nitrogen in dark. The mixture was stirred at room temperature for 1.5 h. After removal of THF under reduced pressure, the crude residue was purified by silica gel column chromatography eluting with $CHCl_3$/MeOH (25:1 to 25:2 to 25:3) to provide pure **5** as a colorless oil. Yield 180 mg, 76.5%; ^{1}H NMR (500 MHz, $CDCl_3$): δ 8.10 (1H, br s, NH), 8.07 (1H, s, 6-H), 6.25 (1H, t, J = 6.8 Hz, 1′-H), 5.32–5.25 (3H, m, 4″-H, 2″-H, 3″-H), 4.63–4.61 (1H, m, 3′-H), 4.83 (1H, d, J = 2.0 Hz, 1″-H), 4.27 (1H, dd, J = 5.5, 12.0 Hz, 6″-$H_{pro\,R}$), 4.15 (1H, dd, J = 2.5, 12.0 Hz, 6″-$H_{pro\,S}$), 4.01 (2H, m, 4′, 5′-H), 3.87 (1H, m, 5″-H), 3.73 (1H, m, C1–O–C*H*H), 3.53 (1H, m, C1–O–CH*H*), 2.94 (1H, br, s, OH), 2.78 (1H, br s, OH), 2.48–2.45 (2H, m, 2′-HH), 2.41–2.35 (2H, m, CH_2–CH_2–C*H*$_2$–C≡C), 2.17, 2.11, 2.05, 2.01 (12H, 4s, $OCOCH_3$), and 1.79–1.77 (2H, m, C*H*$_2$–CH_2–CH_2–C≡C), 1.67–1.64 ppm (2H, m, CH_2–C*H*$_2$–CH_2–C≡C).

5.7. 5-((2,3,4,6-Tetra-*O*-acetyl-α-D-mannopyranosiloxy)-hexyn-1-yl)-2′-deoxy-5′-*O*-(4,4′-dimethoxytrityl)-uridine (6)

4,4′-Dimethoxytritylchloride (0.47 g, 1.38 mmol) was added to a solution of **5** (0.6 g, 0.92 mmol) in 35 mL of dry pyridine under nitrogen in dark. The mixture was stirred at 50 °C for 6 h. The reaction mixture was quenched by addition of water. After cooling to room temperature, the mixture was extracted with CH_2Cl_2 and washed with satd $NaHCO_3$ aq (×3) and water (×2). After drying over anhydrous $MgSO_4$, CH_2Cl_2 was evaporated to provide a thick oil. Purification by silica gel column chromatography eluting with AcOEt/hexane (2:1 to 4:1 to 8:1 containing 0.5 wt % Et_3N) provided pure **6** as a colorless oil. Yield 0.5 g, 56.8%; ^{1}H NMR (500 MHz, $CDCl_3$): δ 7.95 (1H, s, 6-H), 7.15–7.37 (9H, m), 6.76 (4H, d, J = 8.5 Hz), 6.24 (1H, t, J = 6.8 Hz, 1′-H), 5.22–5.14 (4H, m, 4″-H, 2″-H, 3″-H, 3′-H), 4.68 (1H, d, J = 2.0 Hz 1″-H), 3.72 (2H, m, 6″-HH), 4.23–4.20 (1H, m, 4′-H), 4.06–4.00 (1H, m, 5″-H), 3.72 (6H, s, 2′OCH_3), 3.44–3.36 (1H, m, C1–O–CH*H*), 3.36–3.35 (1H, m, C1–O–C*H*H), 3.24–3.18 (2H, m, 5′-HH), 2. 40–2.21 (2H, m, 2′-H), 2.16–2.00 (14H, m, containing singlet at δ 2.08, 2.06, 2.04, 2.03, 4 × $OCOCH_3$, CH_2–CH_2–C*H*$_2$–C≡C), 1.44–1.41 (2H, m, C*H*$_2$–CH_2–CH_2–C≡C), and 1.32–1.19 ppm (2H, m, CH_2–C*H*$_2$–CH_2–C≡C).

5.8. 5-((2,3,4,6-Tetra-*O*-acetyl-α-D-mannopyranosyloxy)-hexyn-1-yl)-2′-deoxy-5′-*O*-(4,4′-dimethoxytrityl)uridine 3′-*O*-(2-cyanoethyl-*N*,*N*,*N*′,*N*′-tetraisopropylphosphor-amidite (7)

1H-Tetrazole (32.9 mg, 0.47 mmol) and 2-cyanoethyl *N*,*N*,*N*′,*N*′-tetraisopropylphosphoramidite (150 mL, 0.47 mmol) were added to a solution of **6** (0.3 g, 0.31 mmol) and MS3A in 12 mL of dry CH_2Cl_2 under argon at −78 °C. The mixture was stirred at room temperature for 6 h. After removal of the molecular sieves by filtration, the filtrate was extracted with AcOEt and washed with satd $NaHCO_3$ aq and brine. After drying over anhydrous $MgSO_4$, AcOEt was evaporated to provide a thick oil. Purification by silica gel column chromatography eluting with AcOEt/hexane (1:1 to 2:1 to 4:1) containing 0.5 wt % Et_3N provided two diastereoisomers of **7** as light yellow foam. Yield 0.3 g, 83.9%; ^{1}H NMR (500 MHz, $CDCl_3$): δ 9.19 (1H, br s, NH), 7.98 (1H, s, 6-H), 7.33–7.16 (9H, m), 6.85–6.82 (4H, m,), 6.30 (1H, t, J = 6.8 Hz, 1′-H), 5.37–5.20 (3H, m, 4″-H, 2″-H, 3″-H), 4.82–4.78 (1H, m, 3′-H), 4.35 (1H, d, J = 2.0 Hz, 1″-H), 4.30–4.12 (3H, m, 6″-HH, 4′-H), 4.00–3.89 (2H, t, J = 6.5 Hz, C1–O–CH_2), 3.79 (6H, s, 2 × OCH_3), 3.87–3.76 (1H, m, 5″-H), 3.52–3.40 (4H, m, 2 × N–CH, OCH_2), 3.36–3.22 (2H, m, 5′-*H*H), 2.61 (2H, t, J = 6.0 Hz, CH_2CN), 2.50–2.42 (2H, m, 2′-H*H*), 2.13–1.99 (14H, m, containing singlet at δ 2.16, 2.11, 2.06, 2.00, 4 × $OCOCH_3$, CH_2–CH_2–C*H*$_2$–C≡C), 1.78–1.75 (2H, m, C*H*$_2$–CH_2–CH_2–C≡C), 1.70–1.66 (2H, m, CH_2–C*H*$_2$–CH_2–C≡C), 1.37 (6H, d, J = 6.5 Hz, $CH(CH_3)_2$), and 1.25 ppm (6H, d, J = 6.0 Hz, $CH(CH_3)_2$).

5.9. Oligodeoxynucleotide synthesis

ODNs were synthesized by automated methods on an Expedite Nucleic Acid Synthesis System using β-cyanoethyl phosphoramidite chemistry in 1.0 μmol scale synthesis cycle. The mannose-modified phosphoramidite **7** was dissolved in dry acetonitrile and loaded onto the machine. Phosphoramidite additions were monitored by release of trityl cation, and the modified phosphoramidite was incorporated to the same extent as the unmodified phosphoramidite (except for the longer coupling time (about twice)). After completion of the synthesis, the oligomers were deprotected by treatment with NH_3 aq at room temperature overnight, which also served to cleave the acetyl groups. Then the protecting

group, salt, and other low-moleculer organic substances were removed with Sephadex NAP-10, and purified by HPLC (eluent: 0.1 M ammonium acetate/CH_3CN = 98:2 to 70:30 for 30 min). After purification all sequence were >99% pure as judged by HPLC.

5.10. CD spectra

Double-strand oligonucleotide samples were prepared by dissolving glycosylated oligonucleotide with an equimolar amount of full complementary or half-sliding complementary ODN at [ODN] = 1.13 μM in PBS. Usually after 1 h, CD spectra of double strand were recorded at 25 °C under equilibrium conditions.

5.11. Melting behaviors

Double-strand ODN samples were prepared by mixing with equimolar amounts of full complementary or half-sliding complementary ODN at [ODN] = 1.13 μM. The absorbance at 260 nm of DNA samples in PBS (pH 7.4) was recorded as a function of rising temperature at 1.0 °C/min on a spectrophotometer equipped with a thermal controller.

5.12. Estimation of molecular sizes of ODN duplexes by SEC

Double-stranded ODN samples were prepared by mixing galactosylated ODN 20-mer with equimolar amounts of full complementary or half-sliding complementary ODNs 20-mer, with 1/2 molar amounts of 40-mer periodic full complementary ODN, and with 1/3 molar amounts of 60-mer periodic full complementary ODN, at [ODN] = 85 μM in PBS (pH 7.4) at 25 °C. Usually after 40 min, the mixture (total 20 μL) of double- and single stranded samples were injected on SEC column and eluted with PBS at 25 °C (flow rate: 0.5 mL/min). Pullulan was used as the molecular weight standard.

5.13. Fluorescence assay for the binding to lectins

To a solution of FITC-labeled ConA and RCA_{120} lectin (14.6 nM, 600 μL) in PBS (pH 7.4) were added 1 μL aliquots of a stock solution of 9.0 mM-ODN sample every 25 min. Fluorescence spectra (500–600 nm) excited at 490 nm were recorded at 25 °C. The change in fluorescence intensity at 520 nm (ΔF) was corrected for the spontaneous quenching of FITC-labeled ConA and RCA_{120} in PBS.

References and notes

1. (a) Fukuda, M.; Hindsgaul, O. *Molecular and Cellular Glycobiology*; Oxford University Press: Oxford, 2000; (b) Varki, A.; Cumming, R.; Esko, J.; Freeze, H.; Hart, G.; Marth, J. *Essentials of Glycobiology*; Cold Spring Harbor Laboratory: New York, 1999.
2. (a) Dwek, R. A. *Chem. Rev.* **1996**, *96*, 683; (b) Lee, Y. C.; Lee, R. T. *Glycoconjugate J.* **2000**, *17*, 543.
3. (a) Lee, Y. C. *FASEB J.* **1992**, *6*, 3193; (b) Mammen, M.; Choi, S. K.; Whitesides, G. M. *Angew. Chem., Int. Ed.* **1998**, *37*, 2754; (c) Lundquist, J. J.; Toone, E. J. *Chem. Rev.* **2002**, *102*, 555.
4. (a) Bovin, N. V. *Glycoconjugate J.* **1998**, *15*, 431; (b) Kiessling, L. L.; Phol, N. L. *Chem. Biol.* **1996**, *3*, 71; (c) Nishimura, S.; Lee, Y. C. In *Polysaccharides*; Dumitriu, S., Ed.; Marcel Dekker: New York, 1998; p 523; (d) Donati, I.; Gamini, A.; Vetere, A.; Campa, C.; Paoletti, S. *Biomacromolecules* **2002**, *3*, 805; (e) David, A.; Kopeckova, P.; Rubinstein, A.; Kopecek, J. *Bioconjugate Chem.* **2001**, *12*, 890; (f) Manning, D. D.; Hu, X.; Kiessling, L. L. *J. Am. Chem. Soc.* **1997**, *119*, 3161; (g) Kamitakahara, H.; Suzuki, T.; Nishigori, N.; Suzuki, Y.; Kanie, O.; Wong, C. H. *Angew. Chem.* **1998**, *110*, 7607; *Angew. Chem., Int. Ed.* **1998**, *37*, 1524.
5. (a) Hasegawa, T.; Kondoh, S.; Matsuura, K.; Kobayashi, K. *Macromolecules* **1999**, *32*, 6595; (b) Tsuchida, A.; Kobayashi, K.; Matsubara, N.; Muramatsu, T.; Suzuki, T.; Suzuki, Y. *Glycoconjugate J.* **1998**, *15*, 1014; (c) Dohi, H.; Nishida, Y.; Mizuno, M.; Shinkai, M.; Kobayashi, T.; Takeda, T.; Uzawa, H.; Kobayashi, K. *Bioorg. Med. Chem.* **1999**, *7*, 2053; (d) Nishida, Y.; Uzawa, H.; Toba, T.; Sasaki, K.; Kondo, H.; Kobayashi, K. *Biomacromolecules* **2000**, *1*, 68; (e) Matsuura, K.; Kitakouji, H.; Sawada, N.; Ishida, H.; Kiso, M.; Kitajima, K.; Kobayshi, K. *J. Am. Chem. Soc.* **2000**, *122*, 7406; (f) Matsuura, K.; Kitakouji, H.; Oda, R.; Morimoto, Y.; Asano, H.; Ishida, H.; Kiso, M.; Kitajima, K.; Kobayshi, K. *Langmuir* **2002**, *18*, 6940; (g) Miura, Y.; Ikeda, T.; Kobayashi, K. *Biomacromolecules* **2003**, *4*, 410.
6. (a) Zanini, D.; Roy, R. *J. Am. Chem. Soc.* **1997**, *119*, 2088; (b) Arce, E.; Nieto, P. M.; Diaz, V.; Castro, R. G.; Bernad, A.; Rojo, J. *Bioconjugate Chem.* **2003**, *14*, 817.
7. (a) Roy, R.; Kim, J. M. *Angew. Chem.* **1999**, *111*, 380; *Angew. Chem., Int. Ed.* **1999**, *38*, 369; (b) Fulton, D. A.; Stoddart, J. F. *Bioconjugate Chem.* **2001**, *12*, 655; (c) Hayashida, O.; Mizuki, K.; Akagi, K.; Matsuo, A.; Kanamori, T.; Nakai, T.; Sando, S.; Aoyama, Y. *J. Am. Chem. Soc.* **2003**, *125*, 594.
8. (a) García-López, J. J.; Hernández-Mateo, F.; Isac-García, J.; Kim, J. M.; Roy, R.; Santoyo-González, F.; Vargas-Berenguel, A. *J. Org. Chem.* **1999**, *64*, 522; (b) Fulton, D. A.; Stoddart, J. F. *Org. Lett.* **2000**, *2*, 1113; (c) Yasuda, N.; Aoki, N.; Abe, H.; Hattori, K. *Chem. Lett.* **2000**, 706; (d) Furuike, T.; Aiba, S.; Nishimura, S. *Tetrahedron* **2000**, *56*, 9909; (e) Nelson, A.; Stoddart, J. F. *Org. Lett.* **2003**, *5*, 3783.
9. (a) Hasegawa, T.; Matsuura, K.; Kobayashi, K. *Chem. Lett.* **2000**, 466; (b) Hasegawa, T.; Yonemura, T.; Matsuura, K.; Kobayashi, K. *Tetrahedron Lett.* **2001**, *42*, 3989; (c) Hasegawa, T.; Yonemura, T.; Matsuura, K.; Kobayashi, K. *Bioconjugate Chem.* **2003**, *14*, 728.
10. Ishikawa, H.; Hara, T.; Arawaki, Y.; Tsuchida, S.; Hosoi, K. *Pharm. Res.* **1990**, *7*, 542.
11. (a) Sato, T.; Serizawa, T.; Ohtake, F.; Nakamura, M.; Terabayashi, T.; Kawanishi, Y.; Okahata, Y. *Biochim. Biophys. Acta* **1998**, *82*, 1380; (b) Hashizume, M.; Sato, T.; Okahata, Y. *Chem. Lett.* **1998**, 399.
12. Kitov, P. I.; Sadowska, J. M.; Mulvey, G.; Armstrong, G. D.; Ling, H.; Pannu, N. S.; Read, R. J.; Bundle, D. R. *Nature* **2000**, *403*, 669.
13. Matsuura, K.; Hibino, M.; Yamada, Y.; Kobayashi, K. *J. Am. Chem. Soc.* **2001**, *123*, 357.
14. Matsuura, K.; Hibino, M.; Ikeda, T.; Yamada, Y.; Kobayashi, K. *Chem. Eur. J.* **2004**, *10*, 352.
15. Matsuura, K.; Hibino, M.; Kataoka, M.; Hayakawa, Y.; Kobayashi, K. *Tetrahedron Lett.* **2000**, *41*, 7529.
16. Hayakawa, Y.; Kataoka, M.; Noyori, R. *J. Org. Chem.* **1996**, *61*, 7996.

17. Sagi, J.; Szemzo, A.; Ebinger, K.; Szabolcos, A.; Sagi, G.; Ruff, E.; Otvos, L. *Tetrahedron Lett.* **1993**, *34*, 2191.
18. Matsuura, K.; Akasaka, T.; Hibino, M.; Kobayashi, K. *Bioconjugate Chem.* **2000**, *11*, 202.
19. Micheisen, U.; Hunter, C. A. *Angew. Chem.* **2000**, *112*, 780; *Angew, Chem. Int. Ed.* **2000**, *39*, 764.
20. Eq. 2 was derived as follows. Consider the hybridization between glyco-ODN A and hsc-ODN B giving alternately prolonged duplex AB. When f is defined as the fraction of hybridized ODN and C as the initial total ODN concentration ($[A]_0 = [B]_0 = C/2$), the degree of association DA and the concentration [A] and [B] at equilibrium are expressed, respectively, by Eqs. 3 and 4.

$$DA = \frac{N_0}{N} = \frac{1}{1-f} \tag{3}$$

$$[A] = [B] = \frac{C(1-f)}{2} \tag{4}$$

where N_0 and N are the total number of ODN molecules present initially and at equilibrium, respectively.
When we assume that multiple equilibria are expressed with an association constant K_{as} for simplicity, we have Eq. 5, which is solved for f ($f < 1$) to yield Eq. 6.

$$K_{as} = \frac{[AB]}{[A][B]} = \frac{2f}{C(1-f)^2} \tag{5}$$

$$f = \frac{CK_{as} + 1 - \sqrt{2CK_{as} + 1}}{CK_{as}} \tag{6}$$

Using Eq. 6, Eq. 3 can be written in Eq. 2.
21. Eq. 2 was described incorrectly in the previous paper (Ref. 14) and the correction has been submitted to *Chem. Eur. J.* **2004**, *10*, 5886. The discussion concerning DA in this paper has been based on the corrected Eq. 2 and Figure 8B.
22. (a) Hardman, K. D.; Ainsworth, C. F. *Biochemistry* **1972**, *11*, 4910; (b) Becker, J. W.; Reeke, G. N., Jr.; Wang, J. L.; Cunningham, B. A.; Edelman, G. M. *J. Biol. Chem.* **1975**, *250*, 1513; (c) Naismith, J. H.; Field, R. A. *J. Biol. Chem.* **1996**, *271*, 972.